Computer "Experiments" on Classical Fluids. IV. Transport Properties and Time-Correlation Functions of the Lennard-Jones Liquid near Its Triple Point

D. Levesque and L. Verlet
*Laboratoire de Physique Théorique et Hautes Energies, Orsay, France**

Juhani Kürkijarvi
University of Helsinki, Finland
(Received 14 September 1972)

A molecular-dynamics "experiment" was performed for a system of 864 particles interacting through a Lennard-Jones potential. The state considered was in the immediate neighborhood of the triple point. The total duration of the "experiment" was quite large: It corresponds to 10^{-9} sec in the case of argon. Transport coefficients were calculated using the standard Kubo formulas. They are compared with the prediction of a simple hard-sphere model. It is shown that, as in the case of the hard-sphere fluid near solidification, the Kubo-correlation function relative to the shear viscosity presents a tail extending at large time. The inclusion of this tail turns out to be essential in explaining the transverse-correlation function and the dynamical-structure factor, which shows, for the lowest wave vectors accessible in this study, a characteristic Brillouin doublet structure. Using the hydrodynamical model of Zwanzig and Bixon, it is shown that the introduction of the long-time tail in the Kubo-correlation function for the viscosity explains the negative plateau of the velocity-autocorrelation function observed near the triple point by Rahman and others.

I. INTRODUCTION

In this paper, we shall report and analyze the results of a computer simulation of argon near its triple point. The aim of this "experiment" was to obtain information on the transport coefficients and the time-dependent correlation functions.

As in the preceding papers of this series[1,2] 864 atoms were considered: enclosed in a cubic box of side L (with periodic boundary conditions). They interact through a Lennard-Jones (LJ) potential

$$V(r) = 4\epsilon[(\sigma/r)^{12} - (\sigma/r)^{6}] . \qquad (1.1)$$

We choose σ, ϵ, and $\tau_0 = (m\sigma/48\epsilon)^{1/2}$ as length, energy, and time units, respectively. When we make a comparison with real argon, we choose $\sigma = 3.405$ Å, $\epsilon = 119.8k_B$, $\tau_0 = 3.112\times10^{-13}$ sec.

Using the method described elsewhere,[1] the integration of the equation of motion was carried out for 100 800 integration steps of $0.032\tau_0$. This corresponds to a total time of 10^{-9} sec in argon. During the integration we calculated the quantities whose time correlation enters in the various Kubo formulas for the transport coefficients. These quantities as well as the coordinates and velocities of the particles are kept on tape.

Section II is devoted to a discussion of the thermodynamics of the state which is considered in this study.

In Sec. III, the results for the shear viscosity, the bulk viscosity, and the thermal conductivity are given. They are interpreted successfully with a hard-sphere model which can be built using the very complete results obtained by Alder, Gass, and Wainwright[3] for the transport coefficients of the hard-sphere gas. The more striking results of this section are the following: The Kubo correlation function for the shear viscosity η presents a tail extending to large times; due to the large incompressibility of the liquid near the triple point, the bulk viscosity ξ tends to be small; because of these two effects, the ratio ξ/η is not of the order of 1 as generally expected, but much smaller, of the order of $\frac{1}{4}$. All these results agree very well with similar properties of the hard-sphere gas near solidification.[3]

We then proceed (Sec. V) to study the correlation of transverse currents. Our results complement with an increased accuracy those obtained by Rahman.[4] They are concentrated in a region of relatively long wavelength, in order to study the generalization of linearized hydrodynamics.[5-8] As a first approximation, we analyze our results in terms of a viscoelastic theory with a k-dependent relaxation time. Shear waves appear as predicted by the theory for $k \gtrsim \sigma^{-1}$ (0.3 Å^{-1} in argon).

The simple viscoelastic theory appears to be inadequate at low wave vectors; it yields shear-wave peaks which are too broad and too low. The more solidlike behavior of the molecular-dynamics results can only be accounted for if one also introduces at finite k's the long-time tail observed at $k = 0$. This tail is described by a second exponential with a large relaxation time. It tends to disappear when k increases and is seen to be related to a collective effect involving a small group of particles.

The dynamical-structure factor $S(k, \omega)$ is then computed and analyzed (Sec. V). It is shown that for $k \lesssim \sigma^{-1}$ this quantity still presents a secondary maximum which is the remainder of the Brillouin doublet as a function of ω. An analysis of the data can be made in terms of three parameters: a frequency-dependent longitudinal viscosity; a k-dependent thermal conductivity; and a k-dependent ratio $\gamma(k)$. Assuming a single-relaxation-time form for the longitudinal viscosity, an excellent fit can be obtained. A disturbing element of this fit is, however, that the limit of $\gamma(k)$ when k goes to zero turns out to be unreasonably large. This failure can be traced back to the neglect of the long-time tail in the generalized viscosity. The inclusion of this tail, as in the transverse case, leads to a completely satisfactory description of the data.

In Sec. V, we reexamine the model which was proposed by Zwanzig and Bixon[9] for the description of the velocity-autocorrelation function. In this model the motion of a LJ molecule was approximated by that of a hard sphere moving in a viscoelastic medium. The constants entering the model are all given by the molecular-dynamics computation. A single-relaxation-time viscoelastic theory leads to results similar to those obtained by Zwanzig. The velocity-autocorrelation function obtained from molecular dynamics is fairly well reproduced, but the model gives rise to oscillations when the "experimental" v.a.f. exhibits a negative plateau at large times. The inclusion of the large-time tail results in a frequency-dependent viscosity coefficient which provides a correct description of the long-time behavior of the velocity-autocorrelation function.

II. THERMODYNAMICAL CONSIDERATIONS

The molecular-dynamics computation reported in this paper has been made for the reduced density $\rho = 0.8442$ and the reduced temperature $T = 0.722$. This state is very near the triple point of the LJ potential[10] which is characterized by $\rho_t = 0.85 \pm 0.01$ and $T_t = 0.68 \pm 0.01$. It is also in the immediate neighborhood of the solidification line; the value of the maximum of the structure factor is equal to 2.76, whereas it reaches the value 2.85 on the solidification line.[10] Using the above-mentioned reduction constant, our state corresponds in argon to $\rho = 1.418$ g/cm^3, $T = 86.5\,^\circ$K. The triple point of argon is quite close: $\rho = 1.435$ g/cm^3, $T = 83.8\,^\circ$K. For our state we obtain for the compressibility factor $P/\rho kT = 0.25$ and for the configurational energy per particle $U_i/N = -6.08$.

We can get the specific heat at constant volume through the fluctuations of the kinetic and potential energy.[11] The first method yields the value 2.6, the other 2.8. We thus choose $c_V = 2.7 \pm 0.1$.

We remark here that, although we have made a computation 100 times longer than most of those usually made for continuous potentials, the error in the specific heat remains of the order of 5%.

The fluctuation of the product of the potential energy and of the virial yields[10]

$$\left(\frac{\partial P}{\partial T}\right)_V = 6.41 \pm 0.2 .$$

We obtain the inverse compressibility by extrapolating the structure factor $S(k)$ computed directly (Sec. V) to zero wave vector. We thus obtain

$$\beta\left(\frac{\partial P}{\partial \rho}\right)_T = 24.7 \pm 0.5 .$$

Using the prolongation procedure described by one of us,[12] with the help of which the complete $g(r)$ from the limited amount of information provided by the molecular-dynamics computation is obtained, we obtain

$$\beta\left(\frac{\partial P}{\partial \rho}\right)_T = 24.0 .$$

Combining these three thermodynamics derivatives, we obtain

$$\gamma = \frac{c_P}{c_V} = 1 + \left(\frac{\partial P}{\partial T}\right)_V^2 \frac{1}{\rho c_V} k_B T \left(\frac{\partial \rho}{\partial P}\right)_V$$
$$= 1.86 \pm 0.1 .$$

From this, we obtain for the speed of sound in reduced units, $c = 0.831$ or $= 906$ m/sec. This is compatible with the experimental value[13] $c = 876$ m/sec. The experimental value for γ is equal to 2.

It is interesting to take this opportunity to examine the predictions of the thermodynamic perturbation theory[14,15] concerning these various thermodynamic derivatives. Using the expressions given in Ref. 15, we obtain

$$c_V = 2.57 , \qquad \gamma = 1.99 ,$$

$$\left(\frac{\partial P}{\partial T}\right)_V = 6.42 , \quad \beta\left(\frac{\partial P}{\partial \rho}\right)_T = 22.6 .$$

III. TRANSPORT COEFFICIENTS

A. Shear Viscosity

The shear viscosity is obtained through the well-known Kubo-like formula

$$\eta = \int_0^\infty \eta(t)\, dt \tag{3.1}$$

with

$$\eta(t) = \frac{\rho}{3k_B T} \sum_G \frac{\langle \tau^{xy}(0)\, \tau^{xy}(t) \rangle}{N} , \tag{3.2}$$

where the sum is to be made on the circular permutation of the indices, and where τ^{xy} component of the microscopic stress tensor given by

$$\tau^{\alpha\beta}(t)=\sum_{i=1}^{i=N}\left(Mv_i^{\alpha}v_i^{\beta}-\frac{1}{2}\sum_{j\neq i}\frac{r_{ij}^{\alpha}r_{ij}^{\beta}}{r_{ij}}\frac{\partial V}{\partial r_{ij}}\right). \tag{3.3}$$

The average over the initial time, indicated by the bracket in (3.2), is done over 27 000 values for the initial time separated by $0.128\tau_0$. The noise level on $\eta(t)$ can be estimated to be about 2–3% of its value for $t=0$, which is equal to the infinite-frequency shear modulus at zero wave vector $G_\infty(0)$. This shear modulus, which can be expressed in terms of the two-body radial-distribution function,[16,17] turns out to be especially simple in the case of the LJ potential, as Zwanzig and Mountain have shown[16]:

$$G_\infty(0)=3P/\rho-\tfrac{24}{5}(U_i/N)-2k_BT\,, \tag{3.4}$$

where P is the pressure and U_i/N is the configurational energy per particle. Using the thermodynamical results given in Sec. I we obtain

$$G_\infty(0)=23.9\,.$$

The evaluation of $\eta(0)$ made using (3.2) yields $\eta(0)=24.7$. The shear viscosity obtained by integrating $\eta(t)$ up to a time of $12.8\tau_0$ is $\eta=27.9\pm2$.

McDonald and Singer[18] have recently calculated the shear viscosity by producing an actual shear on a system of 256 LJ particles.

This method succeeds in calculating the shear viscosity with much less computational effort than in the present paper. It should be noted, however, that this method unavoidably yields a shear viscosity determined for a finite value of the wave length, namely L.

Using the results obtained in Sec. IV, one can understand that these authors obtain a shear viscosity smaller than ours by around 30%.

We shall interpret the value obtained for the shear viscosity with the help of the hard-sphere model already used in the case of the self-diffusion constant.[1] This model was established using preliminary hard-sphere results.[19] Due to the appearance of the more complete and accurate hard-sphere results of Ref. 3, we give here again a detailed explanation of the model. We replace the LJ molecules by hard spheres of diameter d. There is obviously some arbitrariness in choosing this diameter.[20] We find that a good choice consists of taking for the diameter d the value which enables one to fit the equilibrium structure factor $S(k)$ with the analytical hard-sphere structure factor obtained by Wertheim and Thiele as the solution of the PY equation.[21]

For the state we consider, we have $d=1.02$. The packing fraction $\xi=\frac{1}{6}\pi\rho d^3$ is then equal to 0.47. Using the Carnahan–Starling[22] expression for the hard-sphere pressure, we obtain

$$y=(P/\rho k_BT)_{\rm HS}-1=9.7\,.$$

The Enskog mean collision time $\tau_{\rm col}$ can then be obtained. This enables us to connect the scale of time of the hard-sphere gas with that of the LJ molecules:

$$\tau_{\rm col}=(2d/y)(\pi/3T)^{1/2}=0.226\,. \tag{3.5}$$

We see, by the way, that the computation of the LJ transport coefficients which we have made includes 10^7 equivalent hard-sphere collisions. We thus expect the same kind of accuracy as in Alder's longest computations.[3]

The model yields for the diffusion constant

$$D=D^E_{\rm HS}f_D(\xi)\,, \tag{3.6}$$

where $D^E_{\rm HS}$ is the Enskog value for the hard-sphere diffusion constant,

$$D^E_{\rm HS}=\tfrac{1}{32}\,\tau_{\rm col}\,T\,, \tag{3.7}$$

and $f_D(\xi)$ is the correction to the Enskog diffusion constant empirically determined by Alder *et al.*[3] from molecular-dynamics computations on the hard-sphere system. We now apply this model to obtain the diffusion constant of the LJ fluid.[2] We have used in Ref. 2 the preliminary hard-sphere results of Alder and Wainwright.[19] The model yielded diffusion constants which were too large by 20 or 30%. With the new results[3] for $f_D(\xi)$, the discrepancy is reduced to about 10%. In view of the basic roughness of this hard-sphere model it does not make sense to try to improve those results by choosing some other definition of the equivalent hard-sphere diameter.

For the shear viscosity, we found a similar expression

$$\eta=\eta^E_{\rm HS}f_\eta(\xi)\,, \tag{3.8}$$

where $f_\eta(\xi)$ is the empirical correction[3] to the Enskog approximation for the hard-sphere viscosity $\eta^E_{\rm HS}$ which is given by

$$\eta^E_{\rm HS}=(10\,\xi/dy\tau_{\rm col})(1/y+0.8+0.761y)\,. \tag{3.9}$$

For the state considered in this paper, we get $f_\eta(\xi)=1.54$ and $\eta=32.8$. The agreement with the "exact" result is good. The use of the hard-sphere model is seen to overestimate the shear viscosity and to underestimate the diffusion constant.

A consequence of the model is the following: Alder, Gass, and Wainwright[3] have shown that for the hard-sphere gas at high density, Stokes's law with slip boundary conditions holds within 10%. The hard-sphere model, therefore, implies that the Stokes relation also holds for the LJ molecules. It reads, with the present notations,

$$\eta=T/2\pi dD\,. \tag{3.10}$$

For the state under consideration, we have[2] $D=0.0047$. Equation (3.10) gives $\eta=24$, in good

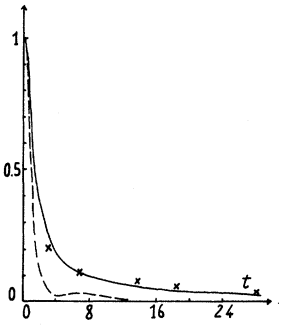

FIG. 1. Solid curve is the function $n_t(0,t)=\eta(t)/\eta(0)$. The crosses are Alder's hard-sphere results for the part of $\eta(t)$ nonlocal in time, the normalization is 1 for $t=0$, and the packing fraction 0.49. The dashed curve is the memory function $n_s(0,t)$ for the autocorrelation function of the velocity at the same LJ state.

agreement with the molecular-dynamics result.

In Fig. 1, we have plotted the function

$$\eta_t(0,t)=\eta(t)/G_\infty(0)\,, \tag{3.11}$$

which is, as we shall see (Sec. IV), the memory function for the transverse-current correlation function at zero wave vector. We see that this function presents a very long tail slowly decaying at large times. We show in Fig. 1, for the sake of comparison, the memory function for the autocorrelation function $n_s(0,t)$ for the same state. As was shown in Ref. 2, this function has a fairly large extension in time which corresponds to the well-known negative-plateau region in the velocity-autocorrelation function near the triple point.[23] The tail of $n_t(0,t)$ is seen to have a different shape and a slower decay.

A long tail in $\eta(t)$ was also observed by Alder, Gass, and Wainwright for the hard-sphere gas near solidification. In Fig. 1 we have shown by crosses the hard-sphere results: they correspond to the part of $\eta(t)$ which is nonlocal in time with a normalization of one for $t=0$. The value of the packing fraction is 0.49. Due to the difference in normalization and packing fraction, the quantitative agreement with the LJ data is coincidental. What we want to emphasize is the remarkable similarity of the slow decay in time. This leads to a large enhancement of the shear viscosity when one gets near solidification.

Using the above-defined hard-sphere model, the value of the packing fraction is a constant along the solidification line. Using (3.5) and (3.9), we thus have

$$\frac{\eta}{\eta_t}=\left(\frac{T}{T_t}\right)^{1/2}\left(\frac{d}{d_t}\right)^{-2}. \tag{3.12}$$

At the triple point of experimental argon we get for the hard-sphere viscosity

$$\eta_t=27.8=3.64\times10^{-3}\ \text{P}\,.$$

Taking into account the variation of d along the solidification line which can be derived using the LJ transition data of Ref. 10, we obtain

$$\eta\simeq\eta_t\,(T/T_t)^{0.63}\,. \tag{3.13}$$

If there is some truth in the hard-sphere model, the experimental situation appears rather puzzling. At the triple point of argon, Boon, Legros, and Thomas[24] obtain $\eta=2.89\times10^{-3}$ P. On the other hand, at a slightly different temperature ($T=88.5$ °K), very close to the transition line, de Bock *et al.*[25] obtain $\eta=3.34\times10^{-3}$ P which, in view of (3.13), would yield a value of 3.25×10^{-3} P for the viscosity of the triple point, in apparent contradiction with the value obtained by Boon *et al.* For the state considered in the present study, these authors give the value $\eta=2.71\times10^{-3}$ P, which differs significantly from the value we obtain for the LJ fluids, i.e., $\eta=3.64\times10^{-3}$ P.

B. Bulk Viscosity

The Kubo formula for the bulk viscosity can be expressed as

$$\xi=\int_0^\infty\xi(t)\,dt\,, \tag{3.14}$$

with

$$\xi(t)=\frac{\rho}{9k_BT}\sum_{\alpha,\beta=1,2,3}\langle[\tau^{\alpha\alpha}(t)-\langle\tau^{\alpha\alpha}\rangle] \times[\tau^{\beta\beta}(0)-\langle\tau^{\beta\beta}\rangle]\rangle\,. \tag{3.15}$$

The function $\xi(t)/\xi(0)$ is plotted in Fig. 2. It is seen that it is a rapidly decreasing function with no appreciable long-time tail. This behavior is in accordance with the hard-sphere results.[3] Zwanzig and Mountain[16] have shown that

$$\xi(0)=K_\infty-K_0\,, \tag{3.16}$$

where K_∞ and K_0 are the infinite and zero-frequency bulk moduli, respectively. For K_∞, we have the relation[16]

$$K_\infty=\tfrac{5}{3}\,G_\infty+2\rho k_B\,T\,(P/\rho k_B\,T-1)=38.7\,. \tag{3.17}$$

For K_0, the adiabatic bulk modulus, we have

$$K_0=\rho\gamma\left(\frac{\partial P}{\partial\rho}\right)_T=28.3\pm2\,. \tag{3.18}$$

We therefore find $K_\infty-K_0=10.4\pm2$, which

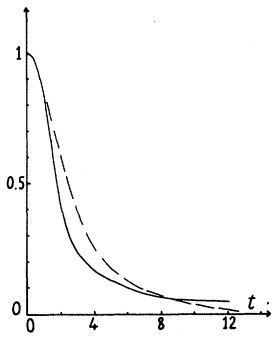

FIG. 2. Solid and dashed curves represent, respectively, $\chi(t)/\chi(0)$ and $K(t)/K(0)$, the normalized Kubo integrands for the bulk viscosity and the heat conductivity (the time unit is 10^{-13} sec).

agrees, within the expected errors, with the result of the molecular-dynamics computation,

$$\xi(0) = 12.3 \pm 1 .$$

The computation also yields $\xi = 7.3 \pm 0.8$, and, therefore, the ratio

$$\xi/\eta = 0.26 \pm 0.05 .$$

For the hard-sphere fluid, Enskog theory gives for that ratio

$$\frac{\xi^E_{\rm HS}}{\eta^E_{\rm HS}} = \frac{1.002y}{0.761y + 0.8 + y^{-1}} . \tag{3.19}$$

We obtain $\xi^E_{\rm HS}/\eta^E_{\rm HS} = 1.1$ for the state considered in this study. This Enskog ratio must be multiplied by the correction factor empirically determined by Alder's group, [3] which for the hard-sphere system near the transition line is of the order of $\frac{1}{4}$. Once again, the hard-sphere model works very well. The low value of ξ/η near the transition line appears to be due to the combination of two factors: the large value of the shear viscosity η owing to the appearance of a long tail in $\eta(t)$ near solidification; the low value of the bulk viscosity, which in the present computation can be related with the appearance of a very high adiabatic bulk modulus when one gets near to the transition line.

This low value of the ratio ξ/η near solidification predicted by the hard-sphere model and "observed" in our computer calculation seems to contradict the existing experiments[13] which yields $\xi/\eta \simeq 0.8$ near the triple point. It would be interesting to have newer, more precise experimental material related to this problem.

C. Thermal Conductivity

The thermal conductivity is given by

$$K = \int_0^\infty K(t)\,dt , \tag{3.20}$$

with

$$K(t) = \langle \mathcal{T}^\alpha_\epsilon(t)\, \mathcal{T}^\alpha_\epsilon(0) \rangle , \tag{3.21}$$

when the energy density flux is given by

$$\mathcal{T}^\alpha_\epsilon(t) = \left(\sum_{i=1}^{i=N} \frac{m v_i^2}{2} + \sum_{i=1}^{i=N} \sum_{j \neq i} \frac{V(r_{ij})}{2} \right) v_i^\alpha - \sum_{i=1}^{i=N} \sum_{j \neq i} \frac{\partial V(r_{ij})}{\partial r_{ij}{}^\alpha} \frac{\vec{r}_{ij} \cdot \vec{v}_i}{2} . \tag{3.22}$$

Due to our use of the expression of the thermal conductivity due to Luttinger, [26] we have made the computation with the last term replaced by

$$-\frac{1}{2} \sum_{i=1}^{i=N} \sum_{j \neq i} [\vec{\nabla} V(r_{ij}) \cdot \vec{r}_{ij}]\, v_i^\alpha .$$

We believe, however, that our results are essentially correct: The contribution of the autocorrelation of this erroneous term to the total heat conductivity is of the order of 0.1%. Its cross terms with the kinetic- and potential-energy fluxes amount to less than 1%. A direct inspection of the corrected terms shows that they should be of the same order, and therefore negligible. Furthermore, we shall see in Sec. V that the extrapolation of the k-dependent heat conductivity which appears in the analysis of $S(k, \omega)$ is in good agreement with the value obtained directly.

$K(t)/K(0)$ is plotted in Fig. 2. As is the case for hard spheres, there appears to be no long tail as a function of time. For the value of the thermal conductivity, we obtain $K = 2.14$.

Using again the hard-sphere model, we obtain in the Enskog approximation

$$K^E_{\rm HS} = \tfrac{25}{32} (\xi/\pi d^2)\, c_V^{\rm HS} (\tfrac{1}{3}\pi T)^{1/2} (1/y + 1.2 + 0.755y) , \tag{3.23}$$

where $c_V^{\rm HS}$ is the hard-sphere specific heat, equal to 1.5.

Making the Alder correction, [3] we obtain

$$K = f_K(\xi) K^E_{\rm HS} = 1.9 .$$

The agreement is quite satisfactory but may be coincidental: it may be argued that we should have tried to apply the hard-sphere model not to K, but rather to the quantity

$$a = K/\rho c_V ,$$

which appears naturally in the theory. In that case, the agreement is completely destroyed.

The comparison with experiment turns out to be disappointing. The molecular-dynamics computation gives

$$a = K/\rho c_V = 0.94$$

$$= 3.5 \times 10^{-3} \text{ cm}^2/\text{sec}.$$

Using the experimental data quoted by Naugle *et al.*, [13] we get

$$a = 1.68 \times 10^{-3} \text{ cm}^2/\text{sec} ,$$

which differs by a factor 2. We may notice that Chung and Yip[6] use, in the analysis of Rahman's[4] computation, the value $a = 3.4 \times 10^{-3}$ cm^2/sec, which agrees very well with ours. The origin of this number is unfortunately not clear.

IV. TRANSVERSE-CURRENTS CORRELATION

The transverse-current correlation function is defined as

$$C_t(k, t) = k^2 \left\langle \sum_{i=1}^{i=N} v_i^x(t)\, e^{-ikz_i(t)} \sum_{j=1}^{i=N} v_j^x(0)\, e^{ikz_j(0)} \right\rangle , \tag{4.1}$$

where $\vec{k}$ is along the z axis.

TABLE I. k is the mean value of the group of vectors $\vec{k}$ considered in the computation of the eight functions $S(k, \omega)$, with the corresponding multiplicity. Δk is the difference between the mean norm of the vector $\vec{k}$ and the norm of the largest or smallest vector of each group.

k	Multiplicity	Δk
0.6235	3	0
0.7526	6	0.13
0.8817	3	0
1.3667	13	0.28
1.9319	19	0.23
2.5348	39	0.28
3.1822	55	0.23
3.8124	72	0.23

Let us introduce its Fourier–Laplace transform:

$$\tilde{C}_t(k, \omega) = \int_0^\infty e^{i\omega t} C_t(k, t)\, dt \ . \tag{4.2}$$

The behavior of $C_t(k, t)$ at small times and the hydrodynamic limit are included through the use of the memory-function formalism.[5–8]

Let us write

$$\tilde{C}_t(k, \omega) = \frac{\omega_0^2}{-i\omega + \omega_t^2 \tilde{n}_t(k, \omega)} \ , \tag{4.3}$$

where

$$\omega_0^2 = C_t(k, 0) \ = k^2 (k_B T/m) \tag{4.4}$$

and[27]

$$\omega_t^2 = \frac{1}{\omega_0^2} \left. \frac{d^2 C_t}{dt^2} \right|_{t=0} = \omega_0^2 + \frac{\rho}{m} \int d\vec{r}\, g(r) \frac{\partial^2 V}{\partial x^2} (1 - e^{ikx})$$

$$= \frac{k^2}{\rho m} G_\infty(k) \ . \tag{4.5}$$

This last equation defines $G_\infty(k)$, the k-dependent shear modulus. In order to obtain the correct hydrodynamic limit, we must have

$$\eta = G_\infty(0) \tilde{n}_t(0, 0). \tag{4.6}$$

The average over initial states implied in (4.1) was made over 33 600 states with an interval of $0.128\tau_0$. $C_t(k, t)$ was calculated for wave vectors whose components were the first multiples of $2\pi/L$.

All the vectors whose length was comprised between k and $k + \Delta k$ were bunched together. The average of k as well as the multiplicity of each group is given in Table I.

We have plotted in Fig. 3 as a function of ω the results of the computation for $\tilde{C}_t(k, \omega)$. We see that, except for the lowest value of the wave vector, $\mathrm{Re}\tilde{C}_t(k, \omega)$ presents a maximum for a nonzero frequency. This is characteristic of the existence of shear waves. If we take for the memory function a simple relaxation form

$$n_t(k, t) = e^{-t/\tau_t(k)} \ , \tag{4.7}$$

it is easy to see that $\mathrm{Re}\tilde{C}_t(k, \omega)$ presents a maximum for ω different from zero if $k > k_c$ where

$$k_c = \left(\frac{m\rho}{2G_\infty(k)} \right)^{1/2} \frac{1}{\tau_t(k)} \ . \tag{4.8}$$

If we neglect the k dependence, we easily get this limiting wave vector. Using (4.6) and (4.7), we have

$$\tau_t(0) = \eta / G_\infty(0) \ = 1.17 \ . \tag{4.9}$$

We see then from (4.8) that shear waves appear when k is larger than $0.79\sigma^{-1}$.

In the relaxation approximation, $\tilde{C}_t(k, \omega)$ depends only, for each value of k, on the parameter $\tau_t(k)$. It is determined from the computer data through a least-squares fit either in the t or the ω variable: The results turn out to be identical. The relaxation times thus obtained are given in Table II and shown in Fig. 4, as circles. We see that the extrapolation to the hydrodynamic limit (4.9) is quite smooth. We have also shown in Fig. 4 the results with crosses of Chung and Yip[6] who have analyzed Rahman's molecular-dynamics computation for the state $\rho = 0.83$, $T = 0.635$. The agreement is seen to be quite good.

In Fig. 3, we compare $\mathrm{Re}\tilde{C}_t(k, \omega)$ obtained in the relaxation approximation with the molecular-dynamics results. We see that the agreement is not very good. In particular, for long wavelengths, the shear-wave peaks are very much flattened out when the relaxation approximation is used. This discrepancy is owing to our neglect of the long-time tail of the memory function $n_t(k, t)$. In order to appreciate the effect of this tail, let us represent the transverse memory function through the two-time exponential formula

$$n_t(k, t) = [1 - \alpha(k)] e^{-t/\tau_<(k)} + \alpha(k) e^{-t/\tau_>} \ . \tag{4.10}$$

We see, using the machine data for $n_t(0, t)$ shown in the Sec. III (Fig. 1), that an excellent fit is ob-

TABLE II. Values of $\tau_t(k)$, $\tau_<(k)$, and $\tau_t'(k)$ in reduced units. The values of $\tau_<(k)$ and $\tau_t'(k)$ given by least-squares fits of $C_t(k, \omega)$ and $S(k, \omega)$ are almost the same. Their difference might be due mostly to the statistical errors of the molecular-dynamics computations.

k	τ_t	$\tau_<$	τ_t'
0	1.17	0.64	0.64
0.7526	0.91	0.70	0.70
1.3667	0.74	0.65	0.58
1.9319	0.66	0.60	0.54
2.5348	0.58	0.54	0.50
3.1822	0.52	0.50	0.45
3.8124	0.46	0.44	0.45

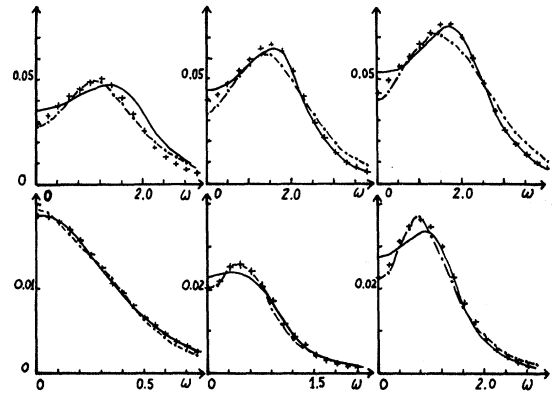

FIG. 3. Transverse-current correlation functions $\mathrm{Re}C_t(k,\omega)/2\pi$ as a function of ω (units τ_0^{-1}). From left to right, and from bottom to top, the six curves are for $k=0.752$, 1.366, 1.931, 2.534, 3.182, and 3.812 (units σ^{-1}). The dash-dot line is the molecular-dynamics results and the solid curve is the relaxation-approximation results. The crosses are the results of the approximation with the memory function (4.10).

tained with $\tau_>=4.72$, $\alpha(0)=0.128$, and

$$\tau_<(0)=[\eta/G_\infty(0)-\alpha\tau_>]/(1-\alpha)=0.63\ .$$

We see the appearance of two times: one $\tau_<$, which is of the order of the molecular-relaxation time, the other $\tau_>$, which is much larger.

We expect that the tail is due to some collective effect. The spatial extension of this tail can be measured through the decay of $\alpha(k)$ and is seen to be of the order of several interparticle distances.

Fitting the molecular dynamics $\tilde{C}_t(k,\omega)$ with the memory function given by (4.10), we obtain the curves shown in Figs. 5 and 6 for $\tau_<(k)$ and $\alpha(k)$. In the latter case, a smooth extrapolation to $k=0$ seems to lead to a value of $\alpha(0)$ which is smaller than 0.128 and may be of the order of 0.1. It can be seen that, given the errors on $C_t(k,t)$, and those, somewhat smaller, affecting $\eta(t)$, there is no real discrepancy there.

We see in Fig. 3 that an excellent fit is obtained for the wave vectors between 1 and 2 σ^{-1}. For the lowest value of k ($k=0.752\sigma^{-1}$), shear waves appear in the model and not in the molecular-dynamics results. This discrepancy is, however, within the computational uncertainties. The presence of

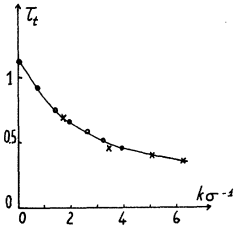

FIG. 4. Single relaxation time $\tau_t(k)$ for the transverse-current correlation function. The circles are our result and the crosses are those of Chung and Yip (Ref. 6) (time in units of τ_0).

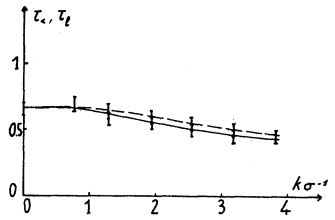

FIG. 5. Short relaxation time in the two-term approximations for the memory function of $n_t(k,t)$ and $n_l(k,t)$. The solid curve is $\tau_l'(k)$, and the dashed curve $\tau_<(k)$ (time in units of τ_0).

the long-time tail lowers the value of the wave vector for which shear waves appear: It is easy to see that in the two-relaxation-time approximation this critical wave vector k_c is determined by solving for the smallest root of

$$\omega_t^4\,\alpha(1-\alpha)\,\tau_>\tau_<(\tau_>-\tau_<)^2 - 2\omega_t^2[\alpha\tau_>^2+(1-\alpha)\,\tau_<^2]+1=0\ ,$$

where ω_t^2 is related to k by (4.5).

We thus obtain $k_c=0.56\sigma^{-1}$ (with $\alpha=0.128$) instead of $k_c=0.78\sigma^{-1}$ in the single-relaxation-time approximation.

The lowering of the value of the critical wave vector is one consequence of the long-time tail. Another consequence, which is more important, is the large enhancement of the shear wave peaks in agreement with the molecular-dynamics experiments. This enhancement may be thought of as a precursory of the solidlike behavior in the neighborhood of the transition line.

For the largest value of k considered here, $\alpha(k)$ is negligible, and the single-relaxation-time approximation is practically recovered. This discrepancy of the fit with molecular dynamics is due to the well-known inadequacy of the exponential memory function which becomes more apparent when the small time region is weighed more, i.e., at high k's. In order to illustrate this statement, we plot in Fig. 7, for the case where $k=0.75\sigma^{-1}$ and $k=3.8\sigma^{-1}$, the memory function directly determined using (3.3). It is compared with the two-exponential approximation (4.10) (dotted curves).

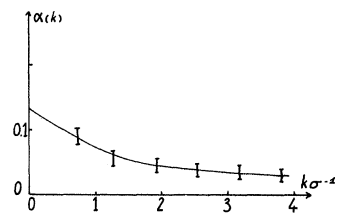

FIG. 6. Coefficient $\alpha(k)$ of the long-time tail of the transverse memory function (4.10).

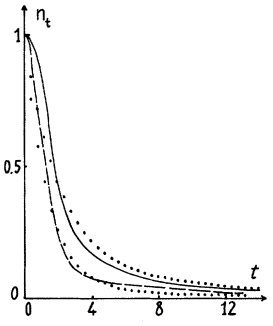

FIG. 7. Memory function $n_t(k,t)$ for $k=0.752\sigma^{-1}$ (solid curve) and $k=3.81\sigma^{-1}$ (dashed curve). Dots are results of the two-exponential approximation (4.10).

V. LONGITUDINAL-CURRENT CORRELATION AND DYNAMICAL-STRUCTURE FACTOR

The longitudinal-current correlation function is given by

$$C_l(k,t)=k^2\left\langle \sum_{i=1}^{i=N} v_i^x(t)\, e^{-ikx_i(t)} \sum_{j=1}^{j=N} v_j^x(0)\, e^{ikx_j(0)} \right\rangle . \tag{5.1}$$

The Fourier–Laplace transform of this function is

$$\tilde{C}_l(k,\omega)=\omega_0^2 \Big/ \left(-i\omega+\frac{\omega_0^2}{-i\omega S(k)}+\tilde{N}_l(k,\omega)\right) , \tag{5.2}$$

where $N_l(k,t)$ is the memory function for longitudinal currents. For small wave vectors and frequency, this must reduce to the hydrodynamical limit[5]

$$\tilde{C}_l(k,\omega)=\omega_0^2 \Big/ \left(-i\omega+\frac{\omega_0^2}{-i\omega S(k)}+D_l k^2 + \frac{\omega_0^2}{S(k)}\,\frac{\gamma-1}{-i\omega+ak^2}\right) , \tag{5.3}$$

with

$$D_l=(1/m\rho)\left(\tfrac{4}{3}\eta+\xi\right) . \tag{5.4}$$

The small-time expansion of $C_l(k,t)$ defines the value of $N_l(k,0)$. A form which includes both this information and the hydrodynamical limit is

$$\tilde{N}_l(k,\omega)=\left(\omega_l^2-\frac{\omega_0^2}{S(k)}\,\gamma(k)\right)\tilde{n}_l(k,\omega) + \frac{\omega_0^2}{S(k)}\,\frac{\gamma(k)-1}{-i\omega+a(k)k^2} , \tag{5.5}$$

with

$$n_l(k,0)=1 . \tag{5.6}$$

For ω_l^2, we have the following expression,[27] in terms of the two-body potential:

$$\omega_l^2=\frac{1}{\omega_0^2}\left.\frac{d^2C_l}{dt^2}\right|_{t=0}=3\omega_0^2+\frac{\rho}{m}\int d\vec{r}\, g(r)\,\frac{\partial^2 V}{\partial z^2}\,(1-e^{ikz}) = \frac{k^2}{\rho m}\left[\tfrac{4}{3}G_\infty(k)+K_\infty(k)\right] . \tag{5.7}$$

This last relation defines $K_\infty(k)$. It reduces to (3.17) for $k=0$. Equation (5.5) includes the assumption that the ω dependence of the generalized thermal conductivity can be neglected.

In terms of the correlation function for longitudinal currents, the dynamical-structure factor is easily obtained as

$$S(k,\omega)=(1/\pi)\,\mathrm{Re}[\tilde{C}_l(k,\omega)/\omega^2] . \tag{5.8}$$

The molecular-dynamics experiments yield the Fourier transform of this function, the so-called intermediate scattering function,

$$F(k,t)=\langle \rho_k(0)\rho_{-k}(t)\rangle/N . \tag{5.9}$$

There, the time average includes 56.000 values for the initial time with a time step of $0.128\tau_0$.

The wave vectors have been grouped as in the transverse case, but with one exception: The lowest group for the transverse currents belonging to $k=0.75\sigma^{-1}$ is the average of two groups of wave vectors of equal lengths $k=0.63\sigma^{-1}$ and $k=0.88\sigma^{-1}$, which are calculated separately in the present case. The results obtained from the computer experiment for $S(k,\omega)$ are shown in Fig. 8. It is seen that, for the smallest wave vectors considered here, there is a secondary peak at finite frequency. Its maximum corresponds to a value of ω/k nearly equal to the macroscopic sound velocity. This structure could be observed experimentally using the long-wavelength neutrons available in high-flux reactors.

As in the transverse case, we first try a simple relaxation approximation by writing

$$\tilde{n}_l(k,\omega)=\frac{1}{-i\omega+1/\tau_l(k)} . \tag{5.10}$$

We can fit the curves of Fig. 8 very well and ob-

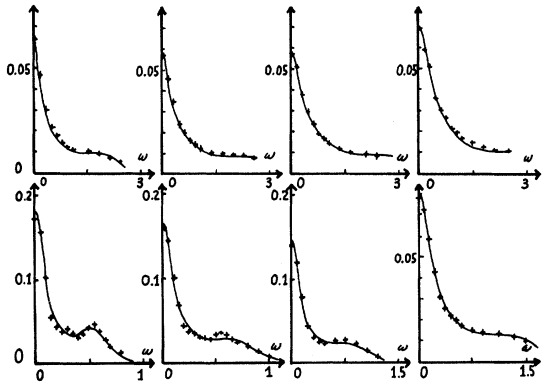

FIG. 8. Function $2S(k,\omega)/\pi$ for eight values of $k=0.623$, 0.752, 0.881, 1.366, 1.931, 2.534, 3.182, and 3.812, from left to right and from bottom to top (units of τ_0^{-1}). The crosses are the molecular-dynamical results and the solid curve is the representation with the memory function $N_l(k,\omega)$ (5.5).

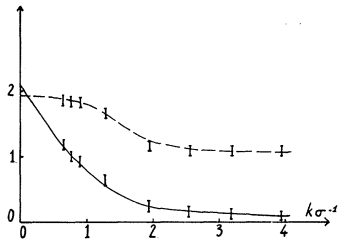

FIG. 9. Dashed curve gives $\gamma(k)$ and the solid curve $a(k)/\rho C_V$ which are two parameters of the memory function $N_l(k,\omega)$. [$a(k)/\rho C_V$ is in reduced units.]

tain the parameters $a(k)$, $\gamma(k)$, and $\tau_l(k)$.

This fit presents some satisfactory aspects: $\tau_l(k)$ tends for large wavelength to its hydrodynamic limit,

$$\tau_l(0) = (\tfrac{4}{3}\eta + \xi)/(\tfrac{4}{3}G_\infty + K_\infty - K_0) \ . \qquad (5.11)$$

The same is true for $a(k)$. Also, when k increases, $\gamma(k)$ tends to 1. This latter quantity, however, behaves quite badly when k is small. For $k = 0.63$, we obtain $\gamma(k) = 2.4$, and the extrapolation of the values obtained through the fit gives $\gamma(0) = 3.4$ instead of the "exact" value $\gamma = 1.86$. If we impose, for the lowest wave vector, a value of $\gamma(k)$ smaller than 2, the fit is completely spoiled.

We can trace this puzzling result to our neglect of the long-time tail which is related to the shear viscosity. Our simplified memory function depends on two times: a first time τ_l which is of the order of 0.6 and another time $1/ak^2$ which for the smaller wave vector is of the order of 3. This second time is substantially larger than the first one. It is of the same magnitude as the long relaxation time $\tau_>$ of the transverse memory function. It appears from these results that the inclusion of the long-time tail in the transverse memory function is necessary. When it is neglected, the fit can only be obtained by artificially raising the coefficient $\gamma(k) - 1$ of the thermal diffusion term: Then due to the similarity in the relaxation times, this term offers, for wave vectors of the order of 0.6, a fair simulation of the tail term which has been neglected.

We shall complete this analysis with the inclusion of the tail term in the longitudinal memory function. Due to the closeness of the bulk relaxation time with $\tau_<(0)$, we can use for the longitudinal memory function the expression

$$n_l(k,t) = [1 - \alpha_l(k)]\, e^{-t/\tau_l'(k)} + \alpha_l(k)\, e^{-t/\tau_>} \qquad (5.12)$$

with

$$\alpha_l(k) = \tfrac{4}{3}\eta(0)\, a(k)/[\tfrac{4}{3}\eta(0) + \xi(0)] \ . \qquad (5.13)$$

The free parameters are now $a(k)$, $\gamma(k)$, and $\tau_l'(k)$. $a(k)/\rho G_V$ is plotted in Fig. 9; we see that it extrapolates correctly to the value of the heat conductivity given in Sec. III. $\gamma(k)$ now tends smoothly to the value $\gamma = 1.86$ which should be reached for $k = 0$. It should be noted that $\gamma(k)$ is practically equal to 1 as soon as k is of the order of 2. The coupling with the thermal modes is then negligible. $\tau_l'(k)$ is very close to $\tau_<(k)$ for all values of k's. These relaxation times have been obtained independently by fitting the longitudinal and transverse correlation function, respectively.

Given the computational uncertainties, the difference between those two relaxation times is not significant. The fit obtained for $S(k,\omega)$ is, on the whole, very good. For the highest values of k considered in this study (k around 3, i.e., of the order of 1 Å^{-1} in argon), there are clear discrepancies for large frequencies. For these relatively high wave vectors the tail term and the heat-coupling term are negligible. We are, therefore, in the rather uninteresting case where a simple memory function, short ranged in time, is sufficient. The discrepancies are due, as in the transverse case, to our use of a memory function of the exponential type, and should be removed by a more careful choice of the shape of that memory function. Much more interesting appears to be the region of lower wave vectors, now accessible with the help of high-flux reactors: it should be possible to observe there the collective effects which we have tried to describe in this paper.

VI. CONNECTION WITH VELOCITY-AUTOCORRELATION FUNCTION

Zwanzig and Bixon[9] have generalized the Stokes expression for the friction constant to finite frequencies. As in the derivation of the Stokes law, the particle whose self-motion is studied is coupled to the medium, described macroscopically, through hard-sphere boundary conditions. In order to calculate the frequency-dependent force acting on the particle, one has to solve the linearized Navier–Stokes equation with transport coefficients generalized to finite frequencies. This can be done analytically if the full coupling with thermal diffusion and the k dependence of the transport coefficients are neglected.

Zwanzig and Bixon have used a simple visco-

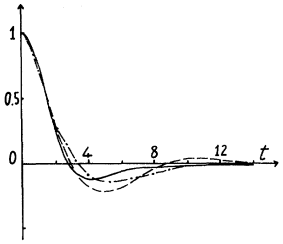

FIG. 10. Autocorrelation function of the velocity (time units 10^{-13} sec) obtained in the Zwanzig–Bixon model (dashed curve), and in the case of the representation (4.10) for $\eta(t)$ (dash-dot curve). The solid curve is the molecular-dynamics results.

elastic theory for the transport coefficient. We repeat their computation because we feel that it is interesting to see what becomes of their result when no parameter at all is adjusted: here, everything is available from the molecular-dynamics computation. As in Sec. III, we choose slip boundary conditions and a hard-sphere diameter chosen to fit the structure factor ($d = 1.02$). The computation involves the isothermal velocity of sound given in Sec. II and the shear and bulk viscosities given in Sec. III. The shear and bulk relaxation times are obtained as $\eta/\eta(0)$ and $\xi/\xi(0)$, respectively. We then obtain the dotted curve of Fig. 10. We see that a surprisingly good agreement is obtained. An important feature is missing: The velocity-autocorrelation function of the LJ fluid near solidification presents an extended negative region, whereas the model leads to oscillations. Zwanzig and Bixon suggest that a more sophisticated frequency dependence of the transport coefficients might remove this discrepancy.

We shall show that this is indeed the case. We keep the same single-relaxation form for the bulk viscosity but use (4.10) to build a frequency-dependent shear viscosity with two relaxation times:

$$\tilde{\eta}(\omega) = \eta\left(\frac{1-\alpha}{1-i\omega\tau_<} + \frac{\alpha}{1-i\omega\tau_>}\right), \qquad (6.1)$$

where $\alpha_1 \tau_>$ and $\tau_<$ are given by (4.11).

Using this expression for the shear viscosity, we obtain the dash-dot curve in Fig. 10. This curve now presents a negative tail at the few percent level which coincides at large times with the molecular-dynamics results. The discrepancies at smaller times are evidently due to the basic roughness of the model. The general agreement appears more remarkable when one tries to vary the parameters of the model. For instance a variation of the shear viscosity by 20% leads to results which are clearly worse than before.

We cannot use a value of α smaller than 0.128, which is as we have seen a rather high value. The results would be improved by increasing that value to 0.15. It is probable that the thermal diffusion which was neglected acts as a supplementary long-wavelength long-time damping which can be simulated by increasing the role of the long-time tail of the shear viscosity a little.

A last remark is the following. For low frequencies, the friction can be represented by

$$\tilde{\gamma}(\omega) = \frac{2\pi d\eta}{m} - \frac{2\pi d^2 i}{3}\left(\frac{i\omega\rho\eta}{m}\right)^{1/2} + O(\omega). \qquad (6.2)$$

As pointed out by Zwanzig and Bixon, due to the square root (6.2), the frequency spectrum of the velocity-autocorrelation function will show a cusp for small ω's. The size of the domain of frequency where this root term predominates determines the extent of the time region when the $t^{-3/2}$ behavior due to this cusp should appear. It is to be noted that the role of the long-time tail in $\eta(t)$ is to reduce very substantially the size of the cusp (it appears only for $\omega \lesssim 0.05$).

The times where the velocity autocorrelation could become positive and behave like $t^{-3/2}$ are, in that case, so high as to lead to completely unobservable effects in a molecular-dynamics computation.

VII. CONCLUSIONS

The study of the LJ fluid near its triple point has demonstrated the existence of a tail extending at large times in the Kubo function which defines the shear viscosity. This tail has observable consequences. First, there should be an enhancement of the shear viscosity and a lowering of the ratio of the bulk to the shear viscosities when one approaches the solidification line. A further and more direct evidence for this tail could be obtained through the analysis of coherent-neutron-scattering experiments to be made with the long-wavelength neutron available with the high-flux reactors.

We are now undertaking a similar study at lower density.

ACKNOWLEDGMENT

The authors had many interesting and stimulating discussions with Professor B. J. Alder.

*Laboratoire associé au Centre National de la Recherche Scientifique. Postal address: Laboratoire de Physique Théorique et Hautes Energies Bâtiment 211, Université Paris Sud, Centre d'Orsay, 91, Orsay, France.

[1]L. Verlet, Phys. Rev. **159**, 98 (1967).
[2]D. Levesque and L. Verlet, Phys. Rev. A **2**, 2514 (1970).
[3]B. J. Alder, D. M. Gass, and T. E. Wainwright, J. Chem. Phys. **53**, 3813 (1970).
[4]A. Rahman, in *Neutron Inelastic Scattering* (International Atomic Energy Agency, Vienna, 1968), Vol. I, p. 561.
[5]L. P. Kadanoff and P. C. Martin, Ann. Phys. (N.Y.) **24**, 419 (1969).
[6]C. H. Chung and S. Yip, Phys. Rev. **182**, 323 (1969).
[7]A. Z. Akcasu and E. Daniels, Phys. Rev. A **2**, 926 (1970).
[8]N. K. Ailawadi, A. Rahman, and R. Zwanzig, Phys. Rev. A **4**, 1616 (1971).
[9]R. Z. Zwanzig and M. Bixon, Phys. Rev. A **2**, 2906 (1970).
[10]J. P. Hansen and L. Verlet, Phys. Rev. **184**, 151 (1969).
[11]J. L. Lebowitz, J. K. Percus, and L. Verlet, Phys. Rev. **153**, 250 (1967).
[12]L. Verlet, Phys. Rev. **165**, 201 (1968).
[13]D. G. Naugle, J. H. Lunsford, and J. R. Singer, J. Chem. Phys. **45**, 4669 (1966).
[14]J. D. Weeks, D. Chandler, and H. C. Andersen, J. Chem. Phys. **54**, 5237 (1971).
[15]L. Verlet and J. J. Weis, Phys. Rev. A **5**, 939 (1972).
[16]R. Zwanzig and R. D. Mountain, J. Chem. Phys. **43**, 4464 (1965).

[17]P. Schofield, Proc. Phys. Soc. Lond. **88,** 149 (1966).
[18]J. Mc Donald and K. Singer (private communication).
[19]B. J. Alder and T. E. Wainwright, Phys. Rev. Lett. **18,** 988 (1967).
[20]M. Ross and P. Schofield, J. Phys. C **4,** L305 (1971).
[21]M. Wertheim, Phys. Rev. Lett. **10,** 321 (1963); E. J. Thiele , J. Chem. Phys. **38,** 1959 (1963).
[22]N. F. Carnahan and K. E. Starling, J. Chem. Phys. **51,** 635 (1969).
[23]A. Rahman, Phys. Rev. A **136,** 405 (1965).
[24]J. P. Boon, J. C. Legros, and G. Thomas, Physica (Utr.) **33,** 547 (1967).
[25]A. de Bock, W. Grevendonk, and W. Herreman, Physica (Utr.) **37,** 227 (1967).
[26]J. M. Luttinger, Phys. Rev. A **135,** 1505 (1964).
[27]P. G. de Gennes, Physica (Utr.) **25,** 825 (1959).

PHYSICAL REVIEW A VOLUME 7, NUMBER 5 MAY 1973

Kinetic Theory of a Dense Gas: Triple-Collision Memory Function*

C. D. Boley and Rashmi C. Desai
Department of Physics, University of Toronto, Toronto M5S 1A7, Ontario, Canada
(Received 3 November 1972; revised manuscript received 15 January 1973)

We study the phase-space density-correlation function $S(\vec{r}\,t;\vec{p}\,\vec{p}')$ for a dense classical gas with repulsive interaction using the language of memory functions. We derive the kinetic equation for S which is valid at all wavelengths and frequencies but limited to second order in the density (triple collisions). This model equation is, on the one hand, an extension of the earlier work of Mazenko to the next order in density and, on the other hand, an extension to arbitrary wavelengths and frequencies of some suggested generalizations of the linearized Boltzmann equation. The memory function for this kinetic equation is shown to be compatible with symmetry properties, sum rules, and the conservation laws. As an illustration of the hydrodynamics, we calculate the shear viscosity and show that the term linear in density agrees with an earlier calculation by Kawasaki and Oppenheim. We also give the analogous kinetic equation for the single-particle correlation function.

I. INTRODUCTION

A growing amount of attention has been focused on the time-dependent fluctuations of a classical many-body system. The principal object of interest is the correlation function

$$S(\vec{r}-\vec{r}',\, t-t';\, \vec{p}\,\vec{p}') = \langle (f(\vec{r}\,\vec{p}t) - \langle f(\vec{r}\,\vec{p}t)\rangle)(f(\vec{r}'\,\vec{p}'t') - \langle f(\vec{r}'\,\vec{p}'t')\rangle)\rangle\,, \tag{1}$$

where $f(\vec{r}\,\vec{p}t)$ is the local density in phase space,

$$f(\vec{r}\,\vec{p}t) = \sum_\alpha \delta(\vec{r}-\vec{r}_\alpha(t))\,\delta(\vec{p}-\vec{p}_\alpha(t))\,, \tag{2}$$

and the sum runs over the particles in the system, with the phase coordinates $(\vec{r}_\alpha, \vec{p}_\alpha)$. The brackets denote a thermal-equilibrium average. Among the interesting quantities which can be determined from S are the neutron- and light-scattering spectra[1,2] and the transport properties. One of the most practical ways of calculating S consists in constructing and solving the appropriate kinetic equation. This equation contains S and the memory function Σ, which accounts for the effects of interparticle collisions. Approximations for S are phrased in terms of approximations to Σ, since the kinetic equation enables one to take into account the secular effects in S due to streaming in phase space. Among the useful approximations to Σ which have appeared recently are a weak-coupling expansion by Akcasu and Duderstadt[3] and Forster and Martin,[4] an expansion to first order in the density n by Mazenko,[5–7] and also a renormalized theory for self-correlations by Mazenko.[8] One of the present authors has pointed out a simple derivation of the low-density memory function.[9]

The calculation of Refs. 3–6 and 9 are either implicitly or explicitly restricted to dilute systems, the weak-coupling memory function being a special case of the low-density memory function. A power-series expansion of Σ to each order in the density is not permissible for all wavelengths and frequencies, since divergent terms would arise from certain events involving four or more particles (in three dimensions).[10] The divergence would begin in the third-order term of Σ. This situation has led to the development of renormalized theories, in which clusters of particles are not isolated but are allowed to interact in an approximate way with the rest of the system. The associated memory functions contain contributions from all orders of the density expansion, and the transport coefficients are not analytic in the density. The early memory functions of this kind were appropriate to relatively dilute systems,[11,12] but that restriction has recently been removed.[8]

Although renormalized theories have the greatest current importance in the theory of dense gases, it is also of some interest to understand the remaining well-behaved terms in the density expansion of Σ. This paper is concerned with that term, which